Journal of New Materials for Electrochemical Systems 16, 089-095 (2013)

Electrochemical Study of a Nano Vesicular Artificial Peroxidase on a Functional Nano Complex Modified Glassy Carbon Electrode

Wei-Yun Yang[1], Jun Hong[1,*], Ying-Xue Zhao[1], Bao-Lin Xiao[1], Yun-Fei Gao[1], Tian Yang[1], Ali Akbar Moosavi-Movahedi[2,†], Hedayatollah Ghourchian[2] and Zainab Moosavi-Movahedi[3]

[1]School of Life Sciences, Henan University, Kaifeng 475000, China
[2]Institute of Biochemistry and Biophysics, University of Tehran, Tehran, Iran
[3]Chemistry & Chemical Engineering Research Center of Iran (CCERCI), Tehran, Iran

Received: December 27, 2012, Accepted: February 21, 2013, Available online: April 08, 2013

Abstract: *A nano vesicular was constructed with the complex consisting of hemin, imidazole Gemini and sodium dodecyl sulfate (SDS) in 50 mM phosphate buffer solution (PBS). The novel nano structure acted as an efficient artificial peroxidase (AP). The AP was also immobilized on a carboxyl functionalized multi-walled carbon nano-tubes (MWCNTs-COOH) and gold nano-particles (AuNPs) nano-complex modified glassy carbon (GC) electrode, with a formal potential of -31± 2 mV vs. Ag/AgCl in 50 mM PBS, at a scan rate of 0.05 Vs^{-1}. The heterogeneous electron transfer constant (ks) was evaluated to be 5.4 ± 0.1s^{-1}. The modified electrode can be used to detect hydrogen peroxide in the range from 0.03 to 160 μM linearly, with a detection limit of 0.03μM. The apparent Michaelis-Menten constant (K_m^{app}) of AP modified electrode was evaluated to be 0.034 ± 0.003mM.*

Keywords: Nano Vesicular; Artificial peroxidase; functional nano complex; hydrogen peroxide; Biosensor

1. INTRODUCTION

Recently, the design of heme proteins have become an active area of research in biochemistry with the aim of delineating the relationships between the structure and function of heme protein catalysis. Artificial peroxidases are designed for practical applications as artificial enzymes and understanding the enzymatic mechanisms. Most peroxidase-like artificial enzymes researches have aimed at the heme structure and the surroundings of the natural heme enzyme [1].

Heme-containing biocatalysts exert their catalytic action through the initial formation of a high-valent-iron-oxo porphyrin intermediate, which is essential for their function. There are many various parameters to affect the redox potential of the heme, such as axial ligand binding to iron in the heme and the hydrophobicity of the heme environment. The relationship between the redox potential and protein structure features may allow predictions to be made regarding the functional properties of the newly designed protein [2-4].

Usually, the electronic properties and biochemical functions of heme prosthetic groups in hemoproteins are relative to the nature of the protein environment surrounding the heme center. The porphyrin macrocycle is coordinated equatorially to the metal center, leaving two axial coordination sites for occupation by amino acid ligand donors from the protein, solvent, or substrate. Previous researchs have shown that porphyrins may be solubilized by detergents through strong hydrophobic interactions between the detergent and the porphyrin at detergent concentrations corresponding to the critical micelle concentration [5-7]. The effect of electrostatic interactions, as hydrophobic effects, can be studied using heme complexes incorporated into micellar solutions with different surface charger[8-11].

Hemoproteins have been studied extensively from mechanistic, kinetics, and thermodynamic properties [12-23].

In the previous study, a nano vesicular structure of artificial peroxidase (AP) with a diameter of about 47 nm was constructed with the complex consisting of heme, imidazole Gemini and sodium dodecyl sulfate (SDS). The mixture of SDS and gemini at a particular concentration provied an apopertein-like hydrophobic

To whom correspondence should be addressed:
*Email: hongjun@henu.edu.cn, Phone: +86-13781161597 Fax: +86-378-3886258
†Email: moosavi@ut.ac.ir

pocket for the heme-imidazole moiet, which produced a peroxidase active site. The catalytic efficienty of the AP was 27% as efficient as the native horseradish peroxidase [20].

In this work, this AP was constructed and immobilized on a nano complex modified glassy carbon (GC) electrode. Electrochemical and electro-catalytic properties of the AP on thus prepared GC electrode were investigated. The AP modified GC electrode could be used as a biosensor (without any protein) for detection of H_2O_2 with good sensitivity and stability.

2. EXPERIMENTAL

2.1. Reagents

Bovine hemin, Iminidazole, L-cysteine (Cys), Nafion (NF, 5% in ethanol), $HAuCl_4$, sodium citrate and sodium dodecyl sulfate (SDS) were obtained from Sigma (Saint Louis, MO, USA), and used without further purification. Gemini (12-2-12, 2Br-) was synthesized and purified according to the literature [24]. Multi-walled carbon nano-tubes (MWCNTs) were purchased from Shenzhen Nanotech Port Ltd. Co. (China). Hydrogen peroxide, sodium dihydrogen phosphate (NaH_2PO_4) and disodium hydrogen phosphate (Na_2HPO_4) were obtained from Shanghai Chemicals Company, China. All solutions were prepared in double-distilled deionized water. Hydrogen peroxide stock solutions were prepared by appropriate dilutions of 30% (v/v) H_2O_2 in de-ionized water. All other chemicals were of analytical grade and used without further purification.

2.2. Apparatus and measurements

Electrochemical studies were carried out in a conventional three-electrode cell powered by an electrochemical system comprising of CHI650C (CHI Instrument, USA). An KCl-saturated Ag/AgCl, a Pt wire and a glassy carbon (GC) electrode of 3 mm diameter (CH Instrument, USA) were used as the reference, counter and working electrodes, respectively. The electrochemical measurements were carried out in N_2-saturated 0.05 M sodium phosphate buffer solution (PBS, pH 7.0) at 25 ± 1°C. Electron macrograph images of samples were obtained using a TEM (JEM-1400, JEOL, Japan) operating at 80 kV. UV-Vis absorption spectra of the AuNPs was obtained on a TU-1901 spectrophotometer (Beijing Purkinje General Instrument Company, China), using a 1 cm path-length cell equipped with a thermostat holder and an external temperature controller (Shanghai Hengping Instrument Company, China) at 25 ± 0.1°C.

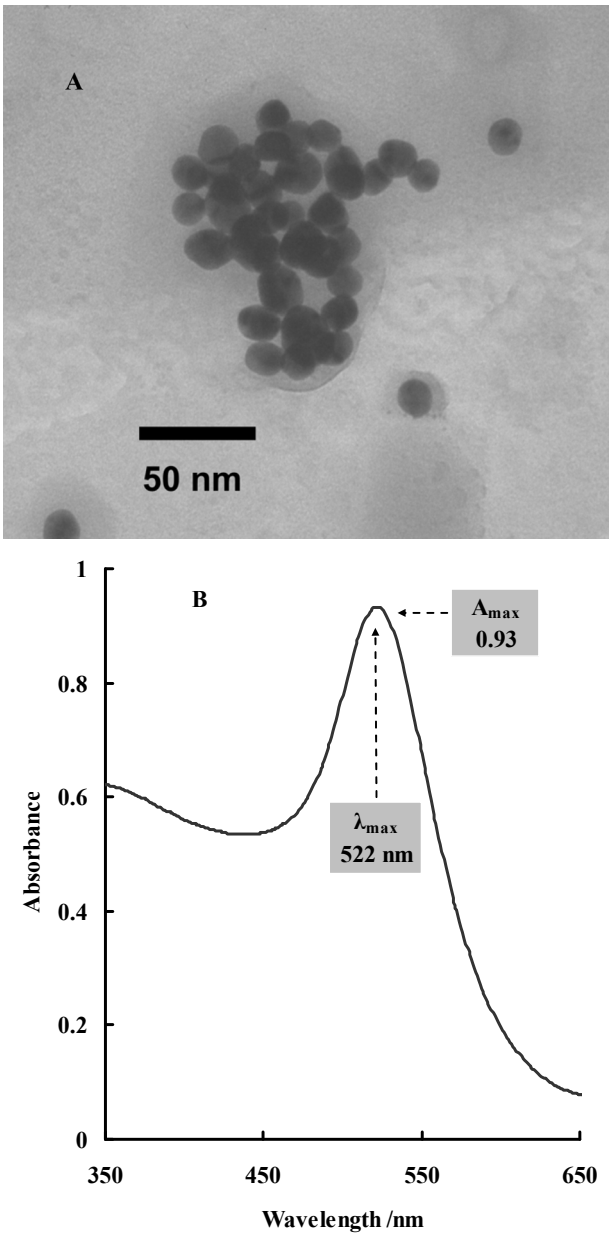

Figure 1. TEM image (A) and UV-vis spectra (B)of AuNPs.

2.3. Preparation of gold nanoparticles (AuPNs)

The preparation of AuPNs was similar to literature [25-27]. Briefly, 0.02 M sodium citrate solution was dropped quickly into the hot $HAuCl_4$ (0.01%) solution, while it was vigorously agitated. It could be seen that at first, the solution color was changed from light yellow to grey, it was then changed to black and gradually to wine red color. When the color did not change anymore, the heating process was stopped and the solution mixture was continuously agitated until it cooled down to room temperature. The prepared AuNPs were stored at 4°C in dark place.

2.4. Carboxylic acid-functionalized MWCNTs (MWCNTs-COOH) preparation

MWCNTs were functionalized according to a previously reported method [28-31]. Briefly, MWCNTs were incubated with a mixture of concentrated H_2SO_4 and HNO_3 (v/v=1/3) under an ultrasonic bath for 4 h at 80°C. The pH value of the solution was then adjusted to 7.0 using NaOH. The MWCNTs-COOH were centrifuged and washed with water three times. The MWCNTs-COOH was then dried at room temperature and examined under transmission electron microscope (TEM).

2.5. AP Preparation

The typical nano vesicular AP was constructed self-assembly by embedding a 10μM heme complex inside the hydrophobic environment of mixed 90 mM SDS, 0.8 mM Gemini (12-2-12, 2Br-) supramolecules containing 3mM imidazole ligands in 50 mM PBS (

pH 7.0)[20]. The mixture was vigorously agitated to form a homogeneous AP solution. And the TEM image of vesicular system has been described in the previous work [20] (not shown in this work). The diameter of the AP was also determined to be about 47 nm by performing dynamic light scattering measurements[20] (not shown in this work).

2.6. Preparation of AP modified glassy carbon electrode

The preparation of the GC electrode was similar to that given in the previous articles [28-32]. Prior to coating, the GC electrode was mechanically polished twice with alumina (particle sizes 1, 0.3 and 0.05 μm, respectively) to a mirror finish. Then, it was treated electrochemically in 200 mM sulfuric acid, cycling between -1.0 and +0.5 V vs. Ag/AgCl at a scan rate of 0.1 V/s for 10 min. And then, the electrode was placed in a 50 mM PBS (pH 7.0), and an anodic potential of 1.7 V vs. Ag/AgCl was applied for 5 min. Then the electrode was washed, and the AuPNs was electro-deposited in the range of 0 - 1.1 V vs. Ag/AgCl at a scan rate of 0.1V/s for 3 min. Then the electrode was dipped in 1mM Cys for 20 min. After washing with water, 3 μl MWCNTs-COOH (2mg/ml) was dropped onto the electrode surface, and then AP (3μl) was dropped on the electrode. After the electrode was dried, 3 μl NF was dropped onto the surface of the electrode to form a protective membrane.

3. RESULTS AND DISCUSSION

3.1. TEM imagine and UV-vis spectrum of AuNPs

The AuNPs were characterized by TEM method, as shown in Figure 1A. The mean diameters of AuNPs could be evaluated to be 18 nm. In order to determine the accuracy of AuNPs mean size, the UV-Vis spectroscopy was also used. Figure 1B shows that the spectrum of prepared AuNPs had a maximum absorption at 522 nm. The average size of AuNPs was then calculated with high accuracy using the Equation (1) [32].

$$d = \left(\frac{A \times 5.89 \times 10^{-6}}{c_{Au} \times \exp(C_1)}\right)^{1/C2} \quad (1)$$

Where, A is the maximum absorption (0.93) and c_{Au} the concentration of Au (0.254 mM here), C_1 = -4.75, C_2 = 0.314, then the mean size of AuNPs (d) was determined to be 18.4 nm[30].

3.2. Redox behavior of AP immobilized on the functional nano complex modified GC electrode

Figure 2 represents the cyclic voltammograms (CVs) of (a) bare GC electrode; (b) NF/MWCNTs-COOH/Cys-AuNPs/GC electrode and (c) NF/AP/MWCNTs-COOH/ Cys-AuNPs /GC electrode at a scan rate of 0.05 V/s. It could be seen that curve (c) shows a pair of well-defined redox wave with the cathodic and anodic peaks at -109 and + 48 mV vs. Ag/AgCl, respectively, then the formal potential (E°') could be calculated to be - 31± 2 mV vs. Ag/AgCl. In the meanwhile, no redox peaks could be seen in curve (a) and curve (b). Moreover, the electrochemical response of AP on bare GC electrode was very weak relative to that of AP on the functional nano complex modified GC electrode (data not shown).

3.3. Electrochemical studies on AP

CVs of NF/AP/MWCNTs-COOH/Cys-AuNPs /GC electrode in 50 mM PBS at various sweep rates were shown in Figure 3A. The peak currents increased with increasing the sweep rate (ν) and were linearly proportional to ν in the range of 0.02–2.0 Vs^{-1} (Figure 3B). The linear regression equations for cathodic and anodic peaks are: $I_{pc}/\mu A = 241.47\nu/(\mu A Vs^{-1}) + 17.403/\mu A$ and $I_{pa}/\mu A = -237\nu/(\mu A Vs^{-1}) - 10.634/\mu A$, respectively. The cyclic voltammograms remained essentially unchanged on consecutive potential cycling, indicating that AP is stably confined on the nano complex modified GC electrode [33,34].

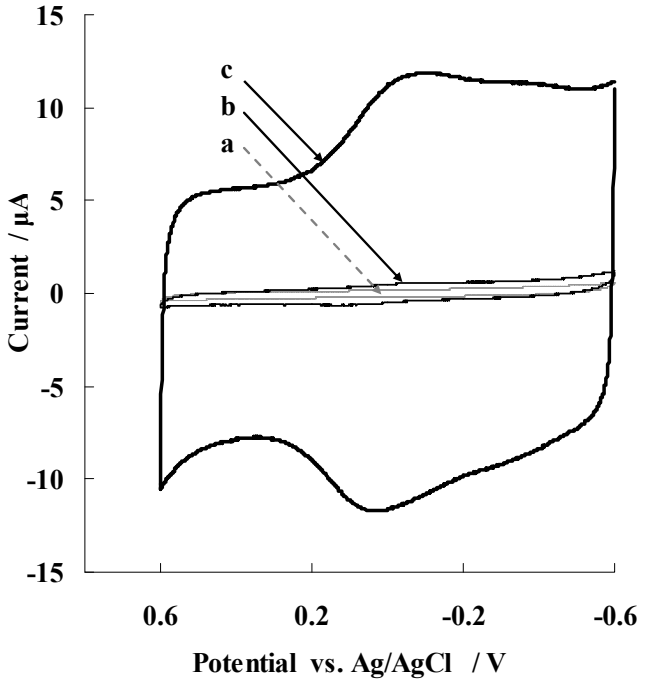

Figure 2. The cyclic voltammograms (CVs) of different modified electrodes: (a) Bare GC electrode, (b) NF/MWCNTs-COOH/Cys-AuNPs/GC electrode, and (c) NF/AP/MWCNTs-COOH/Cys-AuNPs/GC electrode. The experiments were carried out in 0.05 M PBS (pH7.0) at a scan rate of 0.05 Vs^{-1}.

Figure 3C shows the relationship between the peak potential (E_p vs. Ag/AgCl/V) and the natural logarithm of scan rate ($\ln\nu/Vs^{-1}$) for NF/AP/MWCNTs-COOH/ Cys-AuNPs/GC electrode in 50mM PBS (pH 7.0). In the range from 0.3 to 2.0 Vs^{-1}, the cathodic peak potential (E_{pc} vs. Ag/AgCl /V) changed linearly versus $\ln(\nu/Vs^{-1})$ with a linear regression equation of $E_{pc}/V = -0.1927 \ln(\nu/Vs^{-1}) - 0.4445/V$. According to Laviron's Equation (2) [35]:

$$E_p = E^{\circ\prime} + \frac{RT}{\alpha n F} - \frac{RT}{\alpha n F} \ln \nu \quad (2)$$

Where α is the cathodic electron transfer coefficient, n the number of electron, R, F and T are gas, Faraday constant and temperature, respectively (R = 8.314 J $mol^{-1} K^{-1}$, F = 96493 C/mol, T = 298 K). Then αn is calculated to be 0.31. From the general [36], it could be concluded that n = 1 and α =0.31. So, the redox reaction between AP and GC electrode through the nano complex is a single electron transfer process.

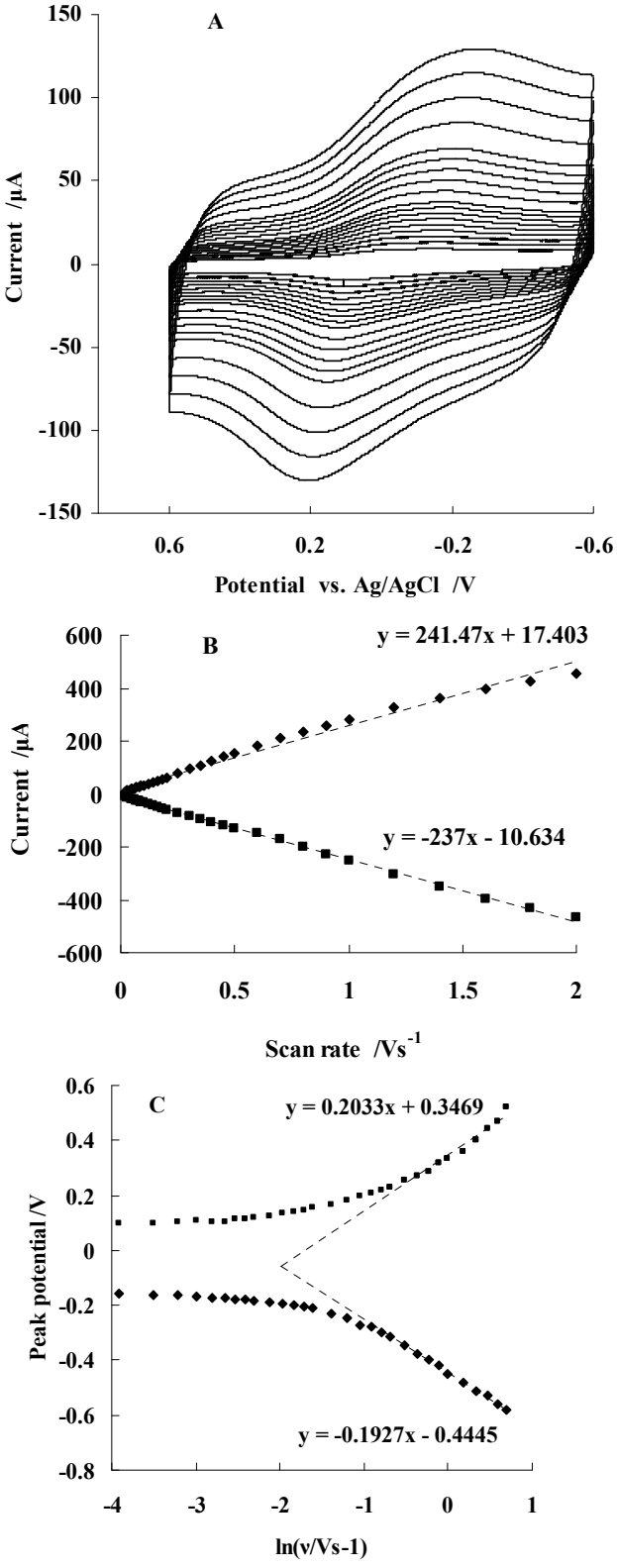

Figure 3. (A) CVs of NF/AP/MWCNTs-COOH/Cys-AuNPs/GC electrode in 0.05 M PBS (pH 7.0) at various scan rates. (B) The relationship between the peak current (I_p/μA) and scan rate (v/Vs^{-1}). (C) The relationship between the peak potential (E_p vs. Ag/AgCl /V) and the natural logarithm of scan rate (lnv/Vs^{-1}).

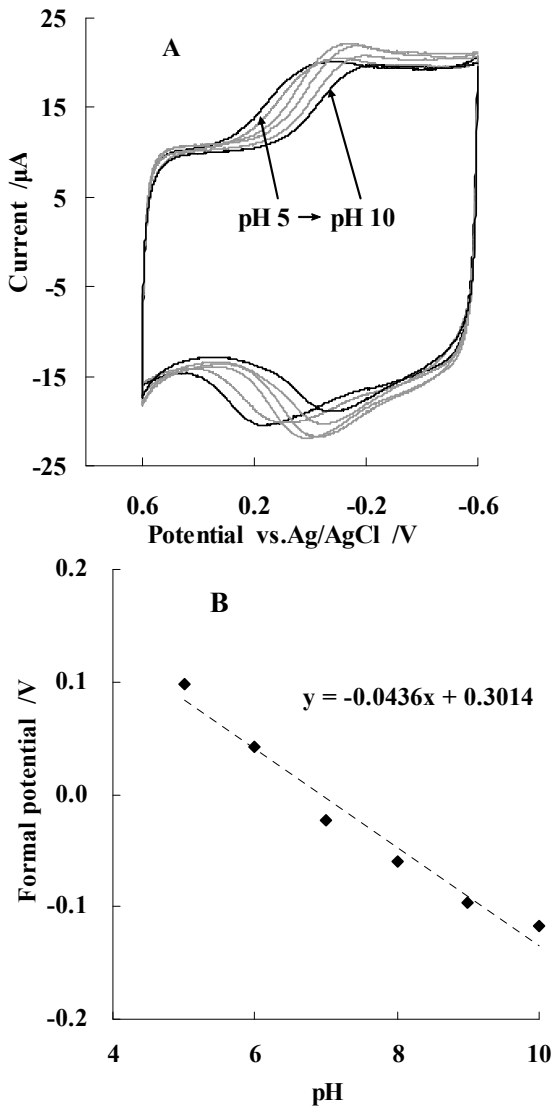

Figure 4. (A) CVs of NF/AP/MWCNTs-COOH/Cys-AuNPs/GC electrode in 0.05M PBS at different pH values (from left to right): 5.0, 6.0, 7.0, 8.0, 9.0 and 10, respectively. (B) The relationship between formal potential ($E^{o'}$ /V) and pH values.

The value of apparent heterogeneous electron transfer rate constant k_s could be calculated using the following equation based on Laviron's Equation (3) [37].

$$\ln k_s = \alpha\ln(1-\alpha) + (1-\alpha)\ln\alpha - \ln\left(\frac{RT}{nFv}\right) - \alpha(1-\alpha)\frac{nF\Delta E_p}{RT} \quad (3)$$

Then the k_s was calculated to be 5.4±0.1 s^{-1}.

The average surface concentration (Γ) of electro-active (heme group) of AP on the surface of GC electrode could be estimated based on the slope of I_p/μA vs.v/Vs^{-1} in the Equation (4) [28-31].

$$I_p = \frac{n^2F^2vA\Gamma}{4RT} \quad (4)$$

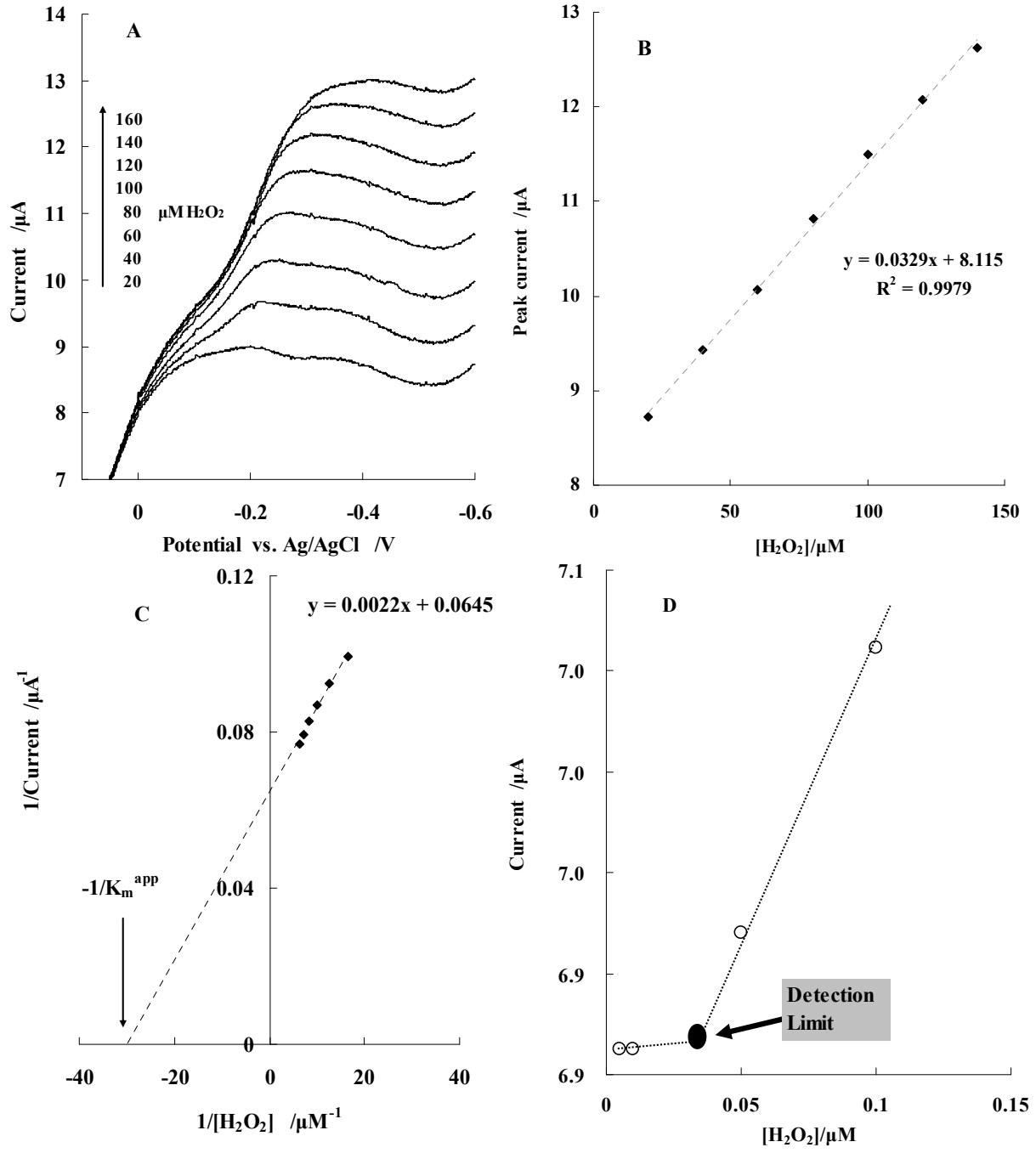

Figure 5. (A) LSVs of NF/AP/MWCNTs-COOH/ Cys-AuNPs /GC electrode in the absence or presence of different concentrations of H_2O_2 (from lower to upper): 20, 40, 60, 80, 100, 120, 140 and 160 μM, respectively. (B) The relationship between the peak current (I_p) and the concentration of H_2O_2 (with the typical linear range from 20 to 160μM). (C) Lineweaver-Burk plot of AP. And (D) Detection limit for the NF/AP/MWCNTs-COOH/ Cys-AuNPs modified GC electrode. The detection limit was determined from the cross point of the lines fitted to the linear segments of the peak current versus the concentration of H_2O_2 ($[H_2O_2]$).

Where I_p is the reduction peak current and A is the electrode surface area. Here, ν = 0.05 V/s, I_p =1.19×10^{-5} A, n=1, A = 7.06×10^{-2} cm^2, F = 96493 C/mol, R = 8.314 J mol^{-1} K^{-1} and T = 298 K, then the value of Γ can be calculated to be 3.59×10^{-9} mol cm^{-2}, which is about 46502-times of the theoretical monolayer coverage of 7.72×10^{-9} mol cm^{-2} (when the diameter of AP was supposed to be 47 nm [20]). This result suggests that nano complex modified on GC electrode helps to confine AP on the electrode.

Moreover, the thickness of NF membrane may also affect the electron transfer process [38-40].

3.4. Effect of pH on the formal potential of the modified GC electrode

Figure 4A represents the CVs of the modified electrode in 50 mM PBS at various pH values. An increase in pH of solution from 5.0 to 10.0 led to a negative shift in both reduction and oxidation peak potentials. Figure 4B shows that the formal potential of the electrode is pH dependent. These results indicated that the slope was 43.6 mV/pH over a pH range from 5.0 to 10.0. This value was less than the ideal Nernst's value of 59.2 mV/pH for one-electron, one-proton process [28-31]. The result might due to the acidic micro-environment provided by NF.

3.5. Biocatalytic activity of the biosensor to H_2O_2

Figure 5A shows the linear sweep voltammograms (LSVs) of NF/AP/ MWCNTs-COOH/Cys-AuNPs /GC electrode in the presence of H_2O_2 (20, 40, 60, 80, 100, 120, 140, 160 μM) at a scan rate of 0.05 Vs^{-1}. The cathodic peak current increased with increased concentration of H_2O_2. Figure 5B represents the relationship between the peak current (I_p) and the concentration of H_2O_2, with the typical linear range from 20 to 160μM.

The apparent Michaelis–Menten constant (K_m^{app}) is a reflection between of both the enzyme affinity and the ratio of microscopic kinetic constants. This value can be obtained from the electrochemical version of the Linewearver–Burk Equation (5) [41,42].

$$\frac{1}{I_{ss}} = \frac{1}{I_{\max}} + \frac{K_m^{app}}{I_{\max} c} \quad (5)$$

Where I_{ss} is the steady-state current after the addition of H_2O_2, c the H_2O_2 concentration in the bulk solution and I_{max} is the maximum current measured under saturated substrate conditions. A low K_m^{app} value indicates a strong substrate binding and exhibits a higher affinity of H_2O_2. Figure 5C shows the Lineweaver-Burk plot for the modified electrode in the presence of different concentrations of H_2O_2. Then the K_m^{app} was calculated to be 0.034±0.003 mM. This value was lower than those reported for HRP immobilized on the modified electrodes of chitosan/sol-gel/GC(6.51 mM) [43], ZrPNsfilm (0.1mM) [44], gelatin–OMIMPF$_6$ modified gold electrode(0.0684mM) [45] and the value reported for the HRP/Au colloid/cysteamine modified electrode (2.3mM) [46]. This value was also much lower than the K_m value of the HPR-modified electrode (5.5mM) [47]. This is an evidence for the higher sensitivity of modified electrode toward H_2O_2.The lower K_m^{app} value indicates a strong substrate binding and exhibits a higher affinity of H_2O_2 for the AP. Furthermore, it should be pointed out that for an AP without any protein, its electro-catalytic properties to H_2O_2 was good.

To determine the detection limit (minimum concentration of H_2O_2 that could be detected by this method), the steady cathodic peak current (Is) of each addition was measured, while the final concentration of H_2O_2 ([H_2O_2]) (from 0.03 μM to 160 μM) was increased gradually. The detection limit was determined to be 0.03 μM from the cross point of lines fitted to the linear segments in the plot of I vs. [H_2O_2] (Figure 5D) [48, 49].

3.6. Stability of the biosensor

Long-term stability is an important parameter for biosensors. The operational stability of the modified electrode was controlled by cyclic voltammetric method. The cathodic peak current and the peak potential was reduced by less than 3% after 50 cycles at a scan rate of 0.05 V/s. The same method was also used to evaluate the storage stability. Almost no change was observed in the CVs after two weeks of electrode storage in PBS at 4ºC (Data not shown).

3.7. Electrochemical studies of the components of AP on the functional nano complex modified GC electrode

To understand the catalytical factor of the each component of AP, the hemin, imidazole Gemini or SDS was modified on the functional nano complex and studied, respectively. The electrochemical parameters for the each component of AP on the functional nano complex modified GC electrode were obtained similarly as the sections of 3.2 and 3.5 of this paper, and are shown in the Table 1. The results here suggested: 1 The SDS and Gemini might be important for the structure of AP. 2. The heme and imidazole might be important for the catalytical function of AP. 3. Both structure and function of AP make it an efficient artificial peroxidase to catalyze the H_2O_2.

4. CONCLUSIONS

A vesicular nano structure artificial peroxidase was constructed and immobilized on a functional nano complex modified GC electrode. Thus prepared AP modified electrode could be used as a biosensor for determination of H_2O_2 with high sensitivity, long-term stability and low detection limit. Moreover, the electrochemical method may be used to analysis the structure and function of AP. The components studies of AP suggested that the SDS and Gemini might be important for the structure of AP, while the heme and imidazole might be important for the catalytical function of AP.

Table 1. Electrochemical parameters of the component of AP on the functional nano complex modified GC electrodes

Component	a	b	c	d	e
Formal potential vs. Ag / AgCl / mV	-31±2	2±2	-50±2	19±2	31±2
K_m^{app} / mM	0.034±0.003	6.62±0.08	16.8±0.5	29.8±0.5	30.8±0.5

a: NF/AP/MWCNTs-COOH/Cys-AuNPs/GC; b: NF/heme/MWCNTs-COOH/Cys-AuNPs/GC; c: NF/SDS/MWCNTs-COOH/Cys-AuNPs/GC; d: NF/Gemini/MWCNTs-COOH/Cys-AuNPs/GC; e: NF/iminidazole/MWCNTs-COOH/Cys-AuNPs/GC
The experiments were carried out in 50 mM PBS (pH 7.0) at a scan rate of 0.05 Vs^{-1}.

5. ACKNOWLEDGEMENTS

Financial support of Henan University Science Foundation, the Research Council of University of Tehran and the Iran National Science Foundation (INSF) is gratefully acknowledged.

REFERENCES

[1] Y. Murakami, J. Kikuchi, Y. Hisaeda, O. Hayashida, Chem. Rev., 96, 721 (1996).

[2] J. Hong, K. Huang, W. Wang, W.Y. Yang, Y.X. Zhao, B.L. Xiao, Z. Moosavi-Movahedi, H. Ghourchian, M. Bohlooli, N. Sheibani, A.A. Moosavi-Movahedi, J. Iran. Chem. Soc., 9, 775 (2012).

[3] T. Arai, K. Ishibashi, K. Tomizaki, T. Kato, N. Nishino, Tetrahedron, 61, 4023 (2005).

[4] A.A. Moosavi-Movahedi, F. Semsarha, H. Heli, K. Nazari, H. Ghourchian, J. Hong, G.H. Hakimelahi, A.A. Saboury, Y. Sefidbakht, Colloid. Surface. A,, 320, 213 (2008).

[5] J.S. Nowick, T. Cao, G. Noronha, J. Am. Chem. Soc., 116, 3285 (1994).

[6] P. Brochette , C. Petit, M.P. Pileni, J. Phys. Chem., 92, 3505 (1988).

[7] H. Fujii, T. Yoshimura, H. Kamada, Inorg. Chem., 36, 6142 (1997).

[8] A.M. Azevedo, V.C. Martins, D.M.F. Prazeres, V. Vojinović, J.M.S. Cabral, L.P. Fonseca, Biotechnol. Ann. Rev., 9, 199 (2003).

[9] X.M. Huang, M. Zhu, H.X. Shen, Microchim. Acta, 128, 87 (1998).

[10]J.K. Tie, W.B Chang, Y.X. Ci, Anal. Chim. Acta, 300, 215 (1995).

[11]S. Nagano, M. Tanaka, K. Ishimore, Biochemistry, 35, 14251 (1996).

[12]R.B. Goodman, R.J. Peanasky, Anal. Biochem., 120, 387 (1982).

[13]K. Buchholz, B. Gödelmann, Biotechnol. Bioeng., 20, 1201 (1978).

[14]T. Tosa, T. Sato, T. Mori, K. Yamamoto, I. Takata, Y. Nishida, I. Chibata, Biotechnol. Bioeng., 21, 1697 (1979).

[15]Y.K. Cho, J.E. Bailey, Biotechnol.Bioeng., 21, 461 (1979).

[16]R. Ohba, H. Chaen, S. Hayashi, S. Ueda, Biotechnol. Bioeng., 20, 665 (1978).

[17]F.A. Armstrong, G. S. Wilson. Electrochim. Acta, 45, 2623 (2000).

[18]S.F. Wang, T. Chen, Z.L. Zhang, X.C. Shen, Z.X. Lu, D.W. Pang, K.Y. Wong, Langmuir, 21, 9260 (2005).

[19]H. Huang, P. He, N. Hu, Y. Zeng, Bioelectrochemistry, 61, 29 (2003).

[20]H. Gharibi, Z. Moosavi-Movahedi, S. Javadian, K. Nazari, A.A. Moosavi-Movahedi, J. Phys. Chem., 115, 4671 (2011).

[21]W. Wang, J. Hong, K. Huang, B.L. Xiao, W.Y. Yang, Y.X. Zhao, Y.F. Gao, Chinese J. Anal. Chem., 40, 1543 (2012).

[22]G. Zhao, Z. Yin, L. Zhang, X. Wei, Electrochem. Commun., 7, 256 (2005).

[23]J. Hong, W. Wang, K. Huang, W.Y. Yang, Y.X. Zhao, B.L. Xiao, Y.F. Gao, Z. Moosavi-Movahedi, S.Ahmadian, M.Bohlooli, A.A.Saboury, H. Ghourchian, N.Sheibani, A.A. Moosavi-Movahedi, Biochem. Engin. J., 65, 16 (2012).

[24]Th. Dam, J.B.F.N. Engberts, J. Karthauser, S. Karaborni, N.M. Van, Colloid. Surface.A., 118, 41 (1996).

[25]M.C. Daniel, D. Astruc, Chem. Rev., 104, 293 (2004).

[26]Y. Xian, Y. Hu, F. Liu, Y. Xian, H. Wang, L. Jin, Biosen. Bioelectron., 21, 1996 (2006).

[27]S.Q. Liu, H.X. Ju, Anal. Biochem., 307, 110 (2002).

[28]K. Huang, J. Hong, W. Wang, B.L. Xiao, Y.X. Zhao, W.Y. Yang, Y.F. Gao, Acta Biophysica Sinica, 28, 773 (2012).

[29]J. Hong, K. Huang, W. Wang, W.Y. Yang, Y.X. Zhao, B.L. Xiao, Z. Moosavi-Movahedi, H. Ghourchian, N. Sheibani, A.A. Moosav-Movahedi., Anal. Lett., 45, 2221 (2012).

[30]J. Hong, W.Y. Yang, Y.X. Zhao, B.L Xiao, Y.F. Gao, T.Yang, H. Ghourchian, Z. Moosavi-Movahedi, N. Sheibani, J.G. Li, A.A. Moosavi-Movahedi. Electrochim.Acta, 89, 317 (2013).

[31]J. Hong, W. Wang, K. Huang, W.Y. Yang, Y.X. Zhao, B.L. Xiao, Y.F. Gao, Z. Moosavi-Movahedi, H. Ghourchian, A.A. Moosavi-Movahedi. Anal.sci., 28, 711 (2012).

[32]W. Haiss, N.T.K. Thanh, J. Aveyard, D.G. Fernig, Anal. Chem. 79, 4215 (2007).

[33]J. Hong, H.Ghourchian, S. Rezaei-Zarchi, A.A. Moosavi-Movahedi, S. Ahmadian, A.A. Saboury, Anal. Lett., 40, 483 (2007).

[34]Y. Tian, L. Mao, T. Okajima, T. Ohsaka, Anal. Chem. 74, 2428 (2002).

[35]E. Laviron, J. Electroanal. Chem. 52, 355 (1974).

[36]H. Ma, N. Hu, J. F. Rusling, Langmuir, 16, 4969 (2000).

[37]E. Laviron, J. Electroanal. Chem. 101, 19 (1979).

[38]H.Yao, N. Li, S. Xu, J.Z. Xu, J.J. Zhu, H.Y. Chen, Biosens. Bioelectron. 21, 372 (2005).

[39]A.E.F. Nassar, Z. Zhang, N. Hu, J.F. Rusling, T.F. Kumosinski, J. Phys.Chem. B, 101, 2224 (1997).

[40]J. Hong, H. Ghourchian, A.A. Moosavi-Movahedi, Electrochem. Commun., 8, 1572 (2006).

[41]Y. Xiao, H.X. Ju, H.Y. Chen, Anal. Biochem., 278, 22 (2000).

[42]R.A. Kamin, G.S. Wilson, Anal. Chem., 52, 1198 (1980).

[43]X.H. Kang, J. Wang, Z.W. Tang, H. Wu, Y.H. Lin, Talanta,78, 120 (2009).

[44]X.S. Yang, X. Chen, L. Yang, W.S. Yang, Bioelectrochemistry, 74, 90 (2008).

[45]R. Yan, F. Zhao, J.W. Li, F. Xiao, S.S. Fan, B.Z. Zeng, Electrochim. Acta, 52, 7425 (2007).

[46]Y. Xiao, H.X. Ju, H.Y. Chen, Anal. Biochem., 278, 22 (2000).

[47]T. Ferri, A. Poscia, R. Santucci, Bioelectrochem. Bioenerg., 45, 221 (1998).

[48]R. P. Buck, E. Linder, Pure Appl. Chem., 66, 2527 (1994).

[49]A. Molaei Rad, H. Ghourchian, A.A. Moosavi-Movahedi, J. Hong, K. Nazari, Anal. Biochem., 362, 38 (2007).